

BOUNDARY LAYER DEPTH MEASUREMENT DISPARITIES DURING THE EVENING TRANSITIONAL PERIOD.

Isaac J. Medina¹, Mentor T. Bell^{2,3}, Mentor Dr. E. Smith², Mentor Dr. J. Carlin^{2,3}

¹National Weather Center Research Experience for Undergraduate Program
Norman, Oklahoma

²NOAA National Severe Storms Laboratory
Norman, Oklahoma

³OU Cooperative Institute for Mesoscale Meteorological Studies
Norman, Oklahoma

ABSTRACT

The planetary boundary layer (PBL) is often under sampled by current operational atmospheric observation methods, especially during the early evening transition (EET). Other methodology such as specialized equipment at the Collaborative Lower Atmospheric Mobile Profiling System (CLAMPS) or dual-polarization NEXRAD radar could provide more consistent PBL measurements. Often, CLAMPS and the radar do not agree on the height of the PBL during the EET. During the EET the radar indication is often much higher than that of CLAMPS's estimates. CLAMPS is better suited to detect the low SBL than the radar as it can use not only kinetic data but also thermodynamic data. The radar searches for areas of high Bragg scatter, which show up as near-zero Z_{DR} to indicate the PBL height. We hypothesize that during the EET, the residual layer's decaying mixing likely dominates any potential Z_{DR} depression signal from the newly forming stable boundary layer—if that stable boundary layer is deep enough for the radar beam to reach it. This study used weather-sensing uncrewed aerial systems (WxUAS) to investigate the character of the layers that these two methods were detecting. These WxUAS data were compared to PBL measurement data collected near Norman Oklahoma on 27 August 2020. With its high-resolution thermodynamic profile measurements, the WxUAS was able to verify that CLAMPS was detecting the SBL, while the radar was seeing an elevated distinctly different layer of the atmosphere. These data were unable to confirm if this layer was a residual layer due to complex structure and lack of continued observation. While this distinct layer may or may not be the residual CBL, it helped contextualize the radar's indications during the EET providing more understanding of the radar-based method's capabilities.

1. INTRODUCTION

During the early evening transition (EET) the planetary boundary layer (PBL) typically undergoes a transition from a daytime convective boundary layer (CBL) to a nocturnal stable boundary layer (SBL).

The CBL has much stronger turbulence with it and develops during the daytime hours (Bonin 2015). This layer has implications on storm development, fog development, and turbulence formation that can have strong impacts on the aviation field (Bonin 2015). Within this layer the air qualities are mixed throughout, meaning the layer's temperate features and atmospheric composition,

including pollutants, are consistent throughout the layer (Bonin 2015). The SBL however, is a low-lying stable layer with weaker turbulence and weaker mixing (Bonin 2015).

Scattering due to fluctuations of atmospheric refractivity on the scale of the radar's wavelength, often associated with turbulence structures such as those present at the top of the CBL is called Bragg scatter, which can be detected in weather radar reflectivity (Melnikov et al. 2013). These returns are due to the Bragg scattering the in atmosphere itself, rather than physical targets, like biota or precipitation. In contrast the SBL does not show high levels of Bragg scatter at its top as the turbulent mixing of the CBL begins to weaken

Corresponding author address: Isaac Medina,
University of Oklahoma, 333 E Brooks St Apt 1206,
Norman, OK 73069, Email: Isaac.j.medina@ou.edu

(Bonin 2015). However, other indicators, such as temperature and water vapor content variations can still be detected using other specialized equipment and used to estimate the height of the SBL or the CBL (Bonin 2015).

Boundary-layer evolution and the EET often go unrecorded due to the infrequent launching of operational radiosondes. These radiosondes are only launched twice a day at 0000 UTC and 1200 UTC at chosen, relatively coarsely spaced locations. This low frequency of data collection can lead to gaps in our understanding of the boundary layer, transitions and associated processes.

A better understanding of the boundary layer can help with research, forecasting, modeling and more. In particular, a better understanding of EET boundary layer can help with our understanding of nocturnal low-level jets (NLLJs) and associated turbulence that impacts the aviation industry. Such applications motivate the need for higher temporal resolution information about boundary layer height. For example, a radar-based method could be implemented on the existing nationwide radar network (NEXRAD) to give continuous and wide-spread coverage information about boundary layer height.

Melnikov et al. (2013) proposed a method using differential reflectivity (Z_{DR}) from dual-polarization radars to estimate boundary layer height and demonstrated a strong correlation between near-zero Z_{DR} values and the high levels of Bragg scatter associated with the CBL top. This was then furthered by Banghoff et al. (2018), which proposed using quasi-vertical profiles (QVPs) to map the diurnal variations of the boundary layer. However, while this current Z_{DR} methodology can successfully detect the CBL, the method is not as accurate compared to reference measurements during the EET.

This study seeks to use specialized boundary-layer instrumentation to contextualize disparities in the radar indicated PBL height during the EET. During a 2020 research mission, concurrent observations are available from the Collaborative Lower Atmospheric Mobile Profiling System (CLAMPS) facilities, a weather-sensing uncrewed aircraft system (WxUAS), and a research WSR-88D (KOUN). The WxUAS is able to travel upward in the atmosphere and continuously collect high resolute data. The profiles returned can be used to analyze the local atmosphere on a parcel scale. This data can then be investigated for thermodynamic indicators of boundary layer height, as these layers have a defined well mixed layer. Therefore, the WxUAS data can be used to verify

the indicated heights of the PBL height estimations from CLAMPS and the KOUN radar.

2. INSTRUMENTATION

The instrumentation used to measure boundary layer height, including the radar detection method and specialized instrumentation are listed below.

2.1 NEXRAD radar

The WSR-88D radar is a dual-polarization radar (a version similar to those in the NEXRAD network) which can return Z_{DR} (Banghoff et al. 2018). The measured Z_{DR} is used to identify areas of high Bragg scatter in the atmosphere (Banghoff et al. 2018).

Generally, the radar scans in a conical pattern, which will return a polar reflectivity scan, referred to as a plan position indicator (PPI) (Banghoff et al. 2018). To generate QVPs, as Banghoff et al. (2018) describes, radar data are first azimuthally averaged, then visualized such that range is converted into height. This method allows for easy analysis of the vertical profile of the atmosphere, which is useful to identify layers of near-zero or otherwise reduced Z_{DR} values.

The algorithm applied herein follows closely to the one proposed by Banghoff et al. (2018), in which the minimum Z_{DR} values, corresponding to areas of Bragg scatter, are identified. In addition, a new smoothing parameter was added that keeps estimates close to the preceding estimates to eliminate unexpected and presumed unphysical variations. This means that our algorithm may not see the minimum Z_{DR} value present, but rather a locally low area.

QVPs from the KOUN radar were used to estimate the height of the PBL. The KOUN radar is located in northern Norman, Oklahoma next to the Max Westheimer Airport. These scans were taken at KOUN during August and September of 2020.

2.2 CLAMPS

CLAMPS is a specialized tool which uses multiple instruments to measure different variables within the lower atmosphere, allowing for a more comprehensive measurement of the boundary layer.

These instruments include a Doppler lidar, an atmospheric emitted radiance interferometer (AERI), and a microwave radiometer, which are all housed in a truck-towed trailer, as seen in Figure 1 (Wagner 2019). The Doppler lidar returns kinetic air



Figure 1. CLAMPS 2 at KAEFS 07/06/2021

movement with both conical scans and vertical stares (Wagner 2019). The AERI and microwave radiometer were both used to return thermodynamic data via a physically based retrieval algorithm (Wagner 2019). This data was then compiled and analyzed using a fuzzy logic algorithm to estimate the boundary layer height. The algorithm weighs turbulent mixing data more heavily during the CBL when the mixing is stronger, and relies more heavily on thermodynamic indicators during the SBL when turbulent mixing is weaker.

During the periods of data collection in August and September of 2020, CLAMPS 1 was located at the Kessler Atmospheric and Ecological Field Station (KAEFS) while CLAMPS 2 was located at KOUN, however CLAMPS 2's microwave radiometer was not functional at this time. KAEFS is located near Washington, Oklahoma south of Norman, Oklahoma.

2.3 WxUAS

The WxUAS can act in similar ways to a controlled radiosonde. The WxUAS, used for this study was the University of Oklahoma's CopterSonde, which can be seen in figure 2. The CopterSonde consists of a rotary winged drone with sensors that can detect and sample wind speed and direction as well as temperature and humidity information (Bell et al. 2020, Segales et al. 2020). The methods of collection as well as sensor information is covered more in depth in Segales et



Figure 2. CASS Coptersonde at KAEFS 07/06/2021

al. 2020. For the purposes of this study, the WxUAS was used in a similar fashion as a radiosonde to compare the radar-indicated PBL height and CLAMPS-indicated PBL height during the evening transition. This was done using the WxUAS data to detect indicators such as temperature or humidity changes that would signify the presence of different layers.

As seen in later figures in the data and results section, the WxUAS data is highly resolute. This means that even compared to a surface based AERI or microwave radiometer, the WxUAS's retrieval can detect more minute changes in the atmosphere. In effect, the WxUAS can sample parcel-scale processes, while radiosondes and profilers are more likely to sample on larger eddy scales.

3. DATA AND ANALYSIS

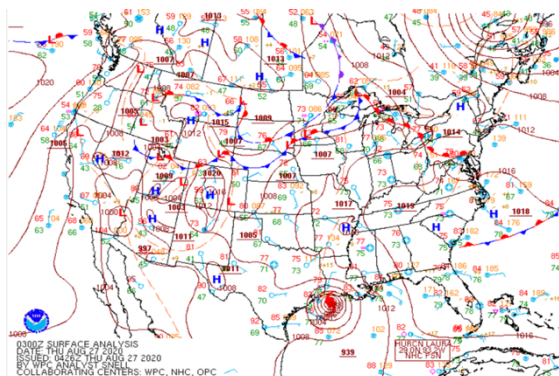


Figure 3. NOAA Surface Analysis 08-27-2020

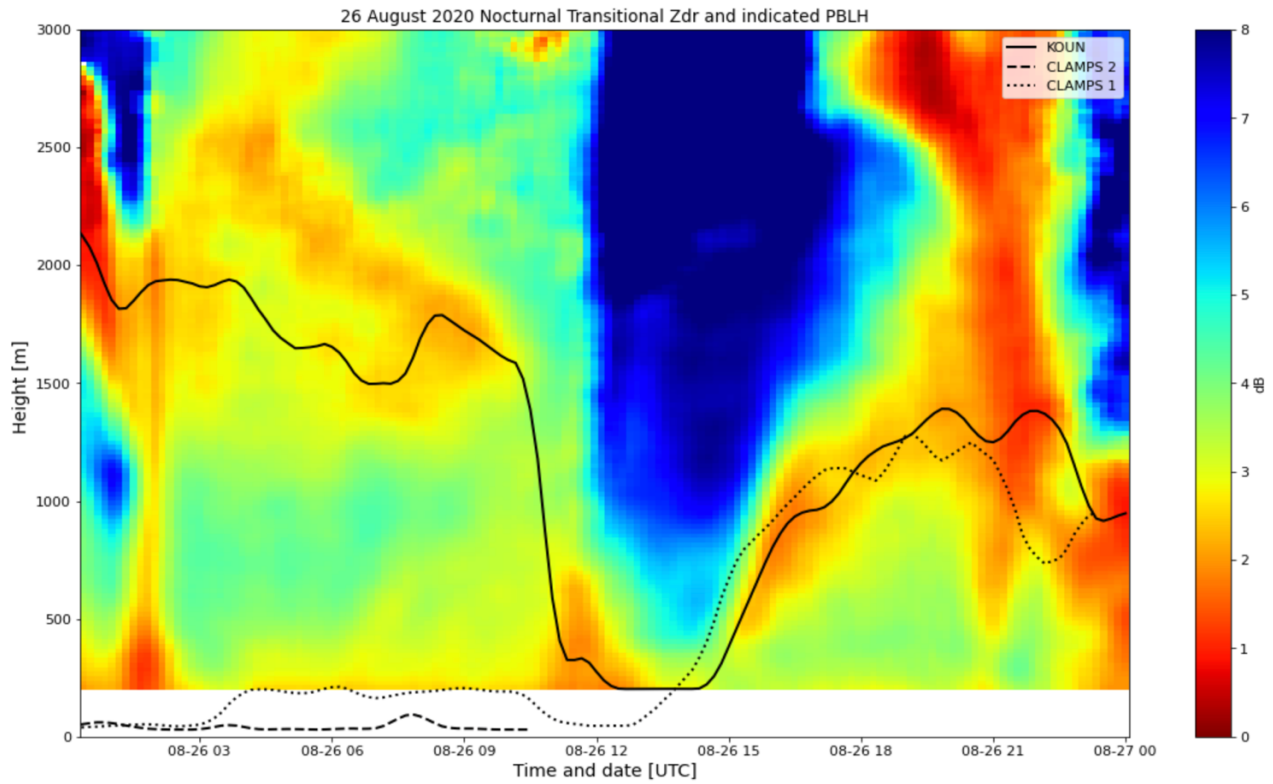


Figure 4. 26 August 2020 KOUN indicated Z_{DR} values with estimated PBL height graphed.

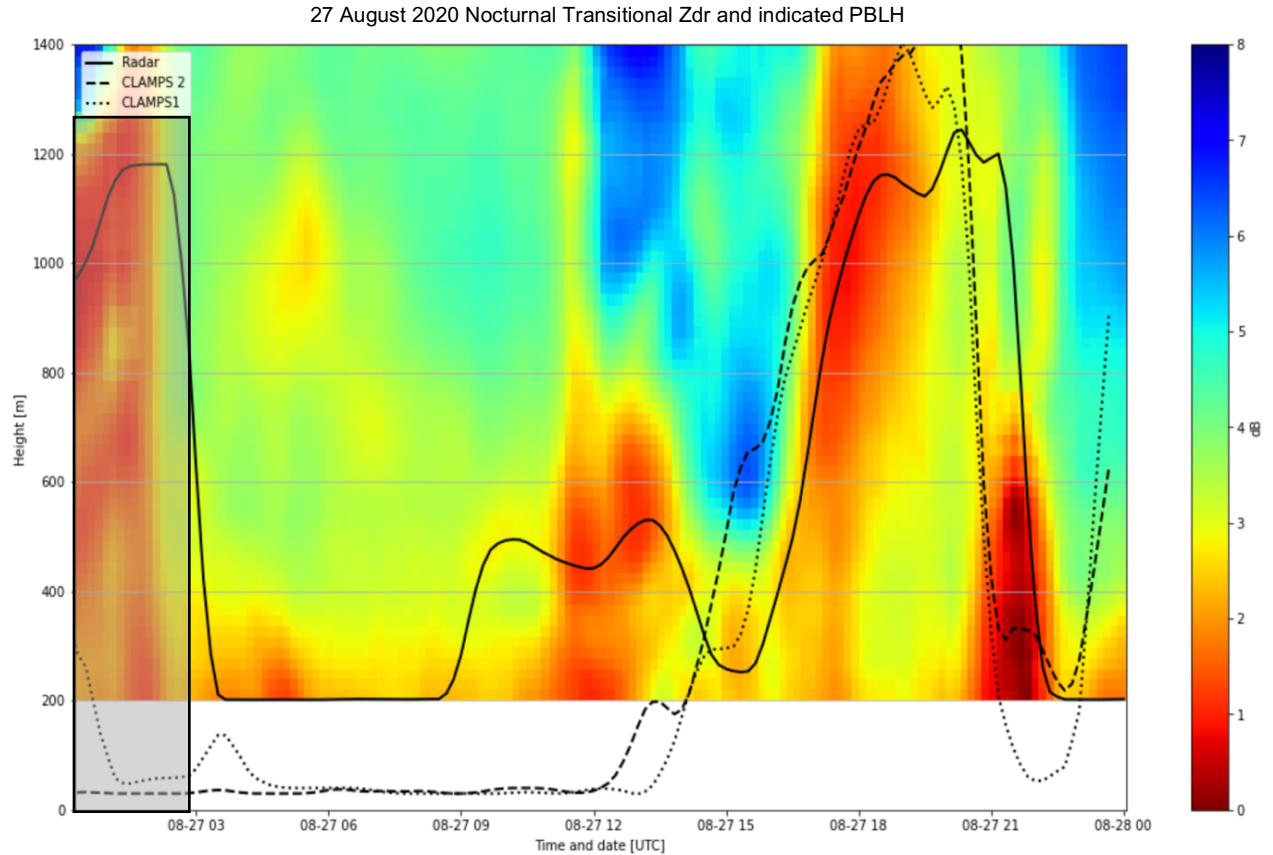


Figure 5. 27 August 2020 KOUN indicated Z_{DR} values with estimated PBL height graphed.

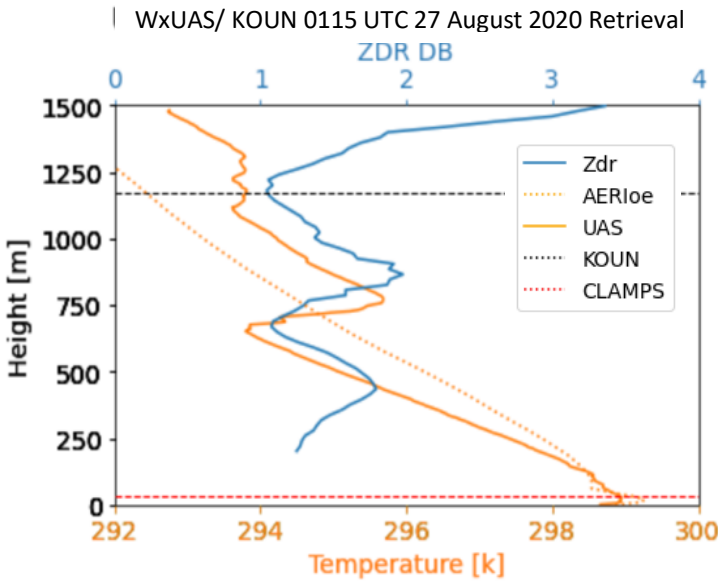


Figure 6. 0115 UTC WxUAS/ AERloe temperature profile. KOUN/ CLAMPS PBL height estimates

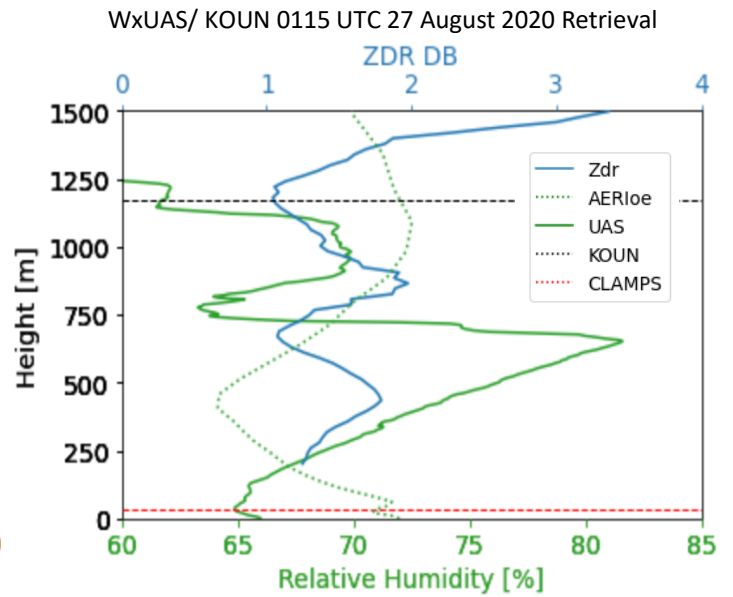


Figure 7. 0115 UTC WxUAS/ AERloe Relative Humidity profile. KOUN/ CLAMPS PBL height estimates

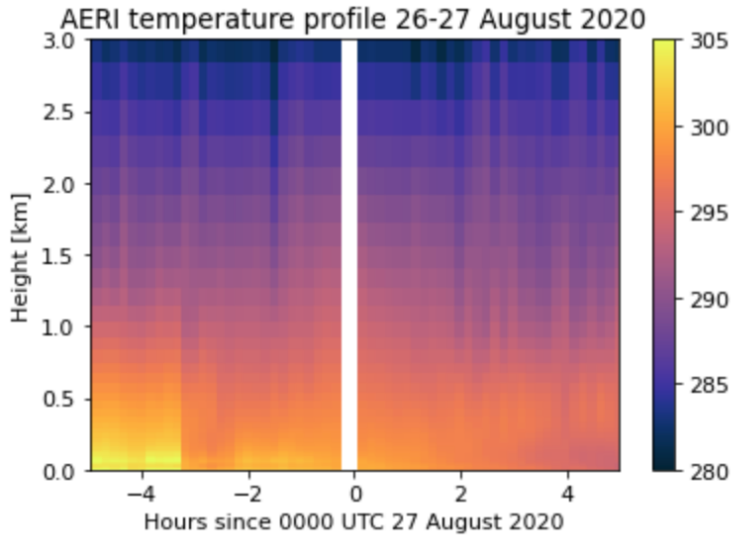


Figure 8. 26- 27 August 2020 AERI retrieved temperature profile

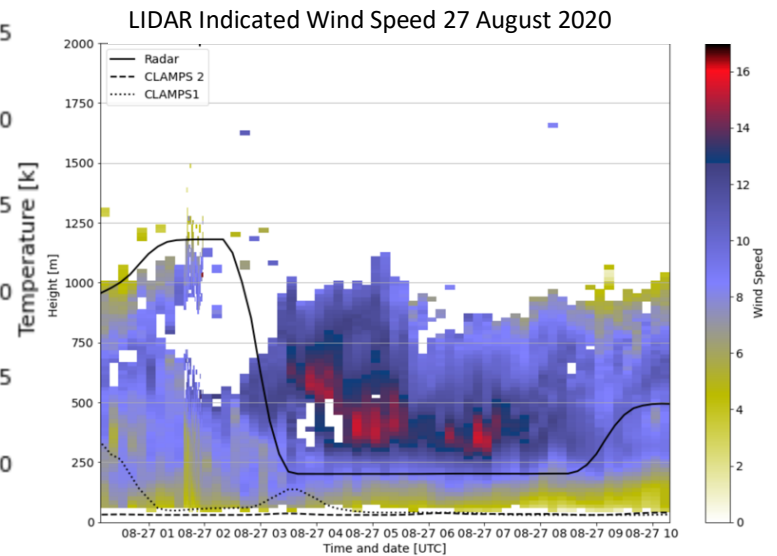


Figure 9. 27 August 2020 LIDAR indicated wind speeds with CLAMPS/ KOUN PBL estimates.

All of the data considered in this study was collected on 27 August 2020 near Norman Oklahoma. Around this time, there was a hurricane moving north from the Louisiana- Texas border, which can be seen in Figure 3. This hurricane would begin to decay and would be located on the Arkansas-Oklahoma border by the end of the day. This decaying storm most likely had impacts on local moisture conditions, as tropically influenced air moved into the area.

On 26-27 August 2020 PBL height as detected by CLAMPS1, CLAMPS2 and KOUN qualitatively agree prior to the EET, seen at the end of figure 4. This is again seen at the end of figure 5 as the CBL grows on 27 August 2020. However, during the EET on 27 August 2020, the end of figure 4 and beginning of figure 5, the KOUN estimated height of the boundary layer remains close to 1200m, while the CLAMPS estimated height of the boundary layer falls to about 50m. This study primarily focuses on this transitional time on 27 August 2020.

Figure 5 has a grey area plotted over this EET disagreement, which shows the period for which WxUAS data is available. This data was used to identify the height of the residual layer and compare that to the radar's boundary layer measurement as well as to provide context to the general disparity between radar and ground-based boundary layer height detection methods during the EET.

The 0115 UTC WxUAS flight temperature, and relative humidity profile are shown in Figures 6 and 7, respectively, alongside Z_{DR} and AERlo_e thermodynamic profiles. The horizontal lines represent KOUN-indicated PBL height (black) and CLAMPS1-indicated PBL height (red; CLAMPS1 was located at the WxUAS flight zone). At 0115 UTC, the WxUAS indicated several layers in which temperature and humidity are well mixed during its upward flight. At the height of the CLAMPS estimate there is a near-surface inversion present in both the WxUAS in-situ and AERlo_e retrieved profiles. This indicates that there is a distinct atmospheric layer present at this height, most likely the nocturnal SBL. This suggests CLAMPS is accurately estimating the boundary layer height.

The WxUAS also indicates a layer of stable temperature and humidity at the same height that KOUN estimated the boundary layer to be present. This again implies that the estimate is valid in detecting a distinct layer, however without data prior to this reading, it is indeterminate if this is the remnants from the CBL from the prior day from WxUAS profiles alone. Without the WxUAS we turn to CLAMPS thermodynamic profiles during this time

to further investigate this layer (Fig. 8). However, the AER-retrieved profiles are not able to provide additional clarity in this case because of the height of the layer of interest. While the AERI does retrieve high-resolution profiles, the effect resolution of these returns deteriorates with height. Therefore, the retrievals above one kilometer lack the fine detail that the WxUAS can obtain and become too coarse to confirm or deny if this layer is in fact a residual layer (Turner and Löhnert 2014).

Later in the night on 27 August 2020 radar PBL height estimates show a rapid decrease around 0300 UTC. Although this is after the period of WxUAS collection, horizontal wind observations from CLAMPS1 show a NLLJ forming at around the same time (Fig. 9). Mechanically-induced turbulence may form below the jet as a result of the high-shear environment near the bottom of the NLLJ (Bonin 2015). Due to the high-shear environment these jets This turbulence can at times be detected by the radar-based PBL height estimation method to reflect this mixing, which looks for these areas of near zero Z_{DR} associated with Bragg scattering in turbulent zones.

However, during this period, there still exists a layer of low Z_{DR} above the NLLJ present in the KOUN returns (Fig. 5). This elevated layer of locally low Z_{DR} may be indicative of the residual layer decaying throughout the night, however, without WxUAS data or other observations to verify this, we cannot be certain. After the NLLJ begins to dissipate, and with it the near-surface mechanical mixing, the radar-based PBLH estimate once again rises to meet the layer hypothesized to be the elevated residual layer. It then tracks this layer until sunrise, at which point it begins to track the new CBL along with CLAMPS.

The overnight hours on 26 August 2020 provide another example of continuously elevated PBL height estimations. The CLAMPS PBL height indication lies near the surface during the transition and throughout the overnight hours while, the radar indicated a PBL height above 1.5 kilometers for a majority of the night (Fig. 4). However, without any verification via WxUAS or other methods, it is difficult to draw conclusions from this case.

4. DISCUSSION

During the period of data collection, a common trend of relatively low Z_{DR} was observed every sunset and sunrise. This trend was also observed to correspond with the brief period between biota blooms seen on the raw PPI scans

from KOUN (Melnikov 2013). These raw scans showed a scan with mixed Z_{DR} values, then a brief absence of increased Z_{DR} values, with a return of them shortly after. Similar signatures were not present in the lidar vertical stares. Due to the difference in wavelength between the lidar and KOUN (i.e., $1.5\mu\text{m}$ and 10 cm , respectively), it may be possible is reasonable to consider that these high Z_{DR} values may be due to insects or other biota which have a relatively high Z_{DR} , as they are large, irregularly shaped scatterers. These areas of low Z_{DR} on the QVP's then can be assumed to be these blooms where biota scatters are temporarily not present during the sunrise or sunset. However, this cannot currently be proven given the scope of the current study, but it would be interesting to look into as this occurrence happens with a high level of consistency.

These daily occurrences were also observed by Banghoff et al. (2018); however, they were not able to confirm what these readings signified. The PPI scans before the bloom (Fig. 10a), during the bloom (Fig. 10b), and after the bloom (Fig. 10c) during sunrise on 27 August 2020 demonstrate the differences in the presence of high Z_{DR} scatters that reflect on the QVPs.

In general, CBL height estimations between from CLAMPS and KOUN approximately agreed throughout daytime periods considered here. The agreement between CLAMPS, designed specifically for measuring boundary layer profiles, and the NEXRAD radar provide further support for the initial findings in Banghoff et al. (2018), Melnikov et al. (2013), and Heinselman et al. (2009).

In all analysis including CLAMPS thermodynamic profile data, only AERloe retrieved data were included. The TROPoe retrieval is also available which includes microwave radiometer data in addition to AERI in the retrieval process. Figs. 11a. and 11b. include TROPoe and AERloe retrieved profiles compared alongside WxUAS profiles of temperature and relative humidity respectively. TROPoe had issues determining atmospheric moisture content. While combining microwave radiometer and AERI data appears to have improved the temperature profile compared to WxUAS and AERloe, the same retrieval showed a bowing disparity around 400m in moisture. Motivated by this comparison, this disparity will be examined in the future with more data collection, where TROPoe can be compared more extensively to WxUAS and AERloe under varying conditions.

While a relationship between the radar-estimated PBL height and boundary layer profile features can be seen within the period of data

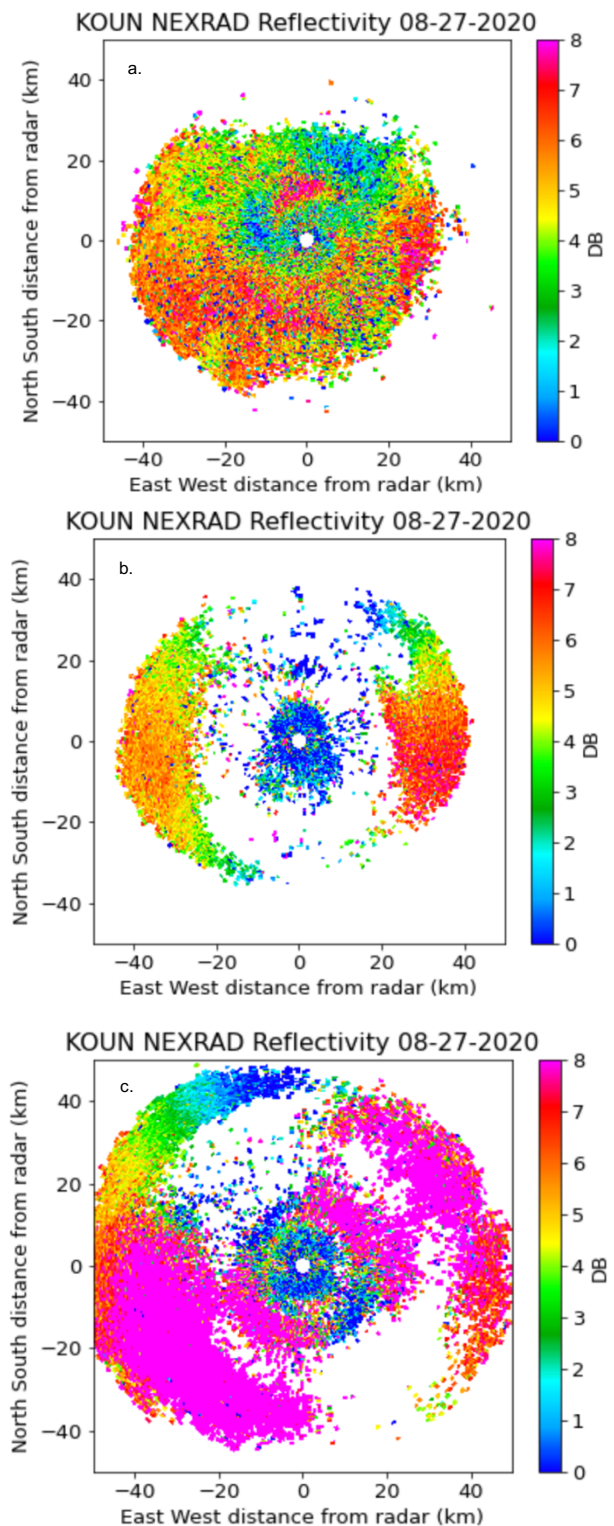


Figure 10. 27 August 2020 KOUN Z_{DR} PPI that show pre-bloom (a.), mid bloom (b.) and post bloom (c.)

collection of this study, the timing of overnight KOUN indications are inconsistent on other nights. On 27 August 2020 KOUN indication's reached its highest nighttime altitude during the EET, while other days saw this happening at other times. Some cases did see an altitude peak during the EET, others saw a spike in indicated altitude around 0400 UTC – 0600 UTC, and other nights, like 26 August 2020, may have seen relatively high indications through the entirety of the overnight period. This inconsistency provides additional challenges in confirming the hypothesis that these disparities are caused by the residual layer.

Cases like those where the radar indicated elevated layers at other times during the nocturnal period would be interesting targets for data collection for going forward. This would require high-altitude WxUAS flights throughout the night, and would help contextualize disparities that might not be caused by an EET boundary layer transition.

As a first step in this direction, we gathered additional cases in May and June of 2021. These additional WxUAS readings were taken at KAEFS in conjunction with both CLAMPS trailers, the PX-1000 radar, and KOUN in Norman. The PX-1000 has a higher temporal and spatial resolution than KOUN (Cheong et al. 2013). With these improvements, the PX-1000 may be able to detect

the SBL better, with readings able to be verified with the collected WxUAS data. This data can be analyzed to provide further contextualization to elevated radar PBL height indications.

5. CONCLUSIONS

This study's use of WxUAS data was able to verify CLAMPS's detection of a shallow stable boundary layer, as well as verify that KOUN was detecting a distinct atmospheric layer at a level above this. However, without additional WxUAS data leading from the end of the daytime CBL through and beyond the EET, it is difficult to be certain that the distinct layer is in fact the residual CBL.

Although these elevated radar-indicated layers are not the lowest portion of the boundary layer present, they are still important to measure. These elevated nocturnal mixing layers may have implications on the height of the next day's capping inversion. These elevated layers are also important to measure as indications of turbulence that may impact the aviation industry, air quality forecasting, and other impactful industries.

Overall, the continued effort to contextualize these results are crucial to understanding the EET, boundary-layer processes, and to promote the potential future inclusion of boundary layer measurements with our current nationwide network of NEXRAD sites. With further cases studied, and new verification methods with existing surface-based instrumentation, we can work to understand what the radar can show in the lower atmosphere. Through continued efforts the NEXRAD network can not only serve as an effective tool for collecting boundary layer height estimates, but it can do so as a large-coverage low-cost option. By implementing a boundary layer detection algorithm to existing sites, it will save the tax-payer money that would be needed to implement more specialized equipment, such as CLAMPS, over a large enough area to compete with the existing network. Such an algorithm would also hold the potential to retroactively analyze historical data on climatological scales.

Acknowledgements. Special thanks to my mentors Dr. Elizabeth Smith, Tyler Bell, and Dr. Jacob Carlin and the support of my friends, without whom this project would not have been possible. This work was prepared by the authors with funding provided by National Science Foundation Grant No. AGS-2050267, and NOAA/Office of Oceanic and Atmospheric Research under NOAA-University of Oklahoma Cooperative Agreement

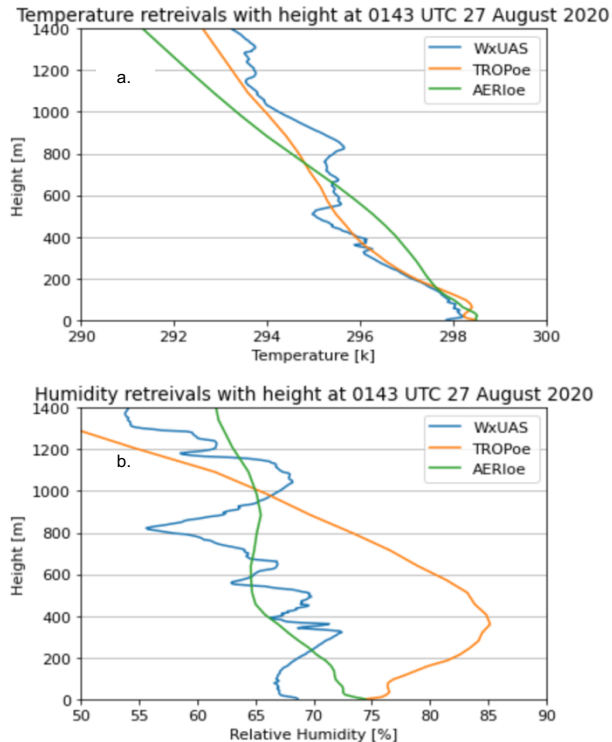


Figure 11. WxUAS, TROPoe, and AERloe temperature (a.) and relative humidity (b.) retrievals at 0143 UTC 27 August 2020,

#NA11OAR4320072, U.S. Department of Commerce. The statements, findings, conclusions, and recommendations are those of the author(s) and do not necessarily reflect the views of the National Science Foundation, NOAA, or the U.S. Department of Commerce. CLAMPS and KOUN data were collected as part of a project supported by the CIMMS Directors Discretionary Research Fund.

Wagner T.J., Klien P.M., Tuner D.D. 2019, New Generation of Ground-Based Mobile Platforms for Active and Passive Profiling of the Boundary Layer, *Bulletin of the American Meteorological Society*, pp 137-152.

REFERENCES

- Banghoff J.R., Stensrud D.J., Kumjian M. R., 2018, Convective Boundary Layer Depth Estimation from S-Band Dual-Polarization Radar, *Journal of Atmospheric and Oceanic Technology*, **35**, 1723-1733
- Bell T.M., Greene B.R., Klein P.M., Carney M., Chilson, P.B., 2020, Confronting the Boundary Layer Data Gap: New and Existing Methodologies of Probing the Lower Atmosphere, *Atmos. Meas. Tech.*, **13**, 3855-3872
- Bonin, T.M., 2015, Nocturnal Boundary Layer and Low-Level Jet Characteristics Under Different Turbulence Regimes. Dissertation, University of Oklahoma, 169.
- Cheong B.L., Kelley R., Palmer R. D., Zhang Y., Yeary M. and Yu T.-Y., PX-1000: A Solid-State Polarimetric X-band Weather Radar and Time-Frequency Multiplexed Waveform for Blind Range Mitigation, *IEEE Trans. Instrum. Meas.*, **62**(11), pp 3064-3072, 2013.
- Heinselman P.L., Stensrud D.J., Hlunchan R.M., Spencer P.L., Burke P.C., Elmore K.L., 2009, Radar Reflectivity-Based Estimates of Mixed Layer Depth, *Journal of Atmospheric and Oceanic Technology*, **26** pp. 229-239.
- Melnikov V.M., Doviak R.J., Znić D.S. Stensrud D.J., 2013. Structures of Bragg Scatter Observed with Polarimetric WSR-88D, *Journal of Atmospheric and Oceanic Technology*, **30**, 1253-1258
- Segales A.R., Greene B.R., Bell T.M., Doyle W., Martin, J.J., Pillar-Little, E.A., Chilson, P.B., 2020, *Atmos. Meas. Tech.*, **13**, 2833-2848
- Turner D.D., Löhnert U. 2014, Information Content and Uncertainties in Thermodynamic Profiles and Liquid Cloud Properties Retrieved from the Ground-Based Atmospheric Emitted Radiance Interferometer (AERI), *Journal of Applied Meteorology and Climatology*, **53**(3), 752-771